Spin polarization dependence of quasiparticle properties in graphene

A. Qaiumzadeh,[1] Kh. Jahanbani,[2,3] and Reza Asgari[2,*]

[1]*Department of Physics, Norwegian University of Science and Technology, NO-7491 Trondheim, Norway*

[2]*School of Physics, Institute for Research in Fundamental Sciences (IPM), Tehran 19395-5531, Iran*

[3]*Institute for Advanced Studies in Basic Sciences (IASBS), Zanjan, P.O. Box 45195-1159, Iran*

(Received 23 January 2012; revised manuscript received 9 April 2012; published 13 June 2012)

We address spin polarization dependence of graphene's Fermi liquid properties quantitatively using a microscopic random phase approximation theory in an interacting spin-polarized Dirac electron system. We show an enhancement of the minority-spin many-body velocity renormalization at fully spin polarization due to reduction in the electron density and consequently increase in the interaction between electrons near the Fermi surface. We also show that the spin dependence of the Fermi velocity in the chiral Fermi systems is different than that in a conventional two-dimensional electron liquid. In addition, we show that the ratio of the majority-to-minority-spin lifetime is smaller than unity and related directly to the polarization and electron energy. The spin-polarization dependence of the carrier Fermi velocity is of significance in various spintronic applications.

DOI: 10.1103/PhysRevB.85.235428 PACS number(s): 71.10.Ay, 72.25.Dc, 73.21.−b, 71.10.−w

I. INTRODUCTION

Graphene is a two-dimensional crystal of carbon atoms, which has been recently discovered.[1] This stable crystal has attracted considerable attention[2] because of its unusual effective many-body properties[3–8] that follow from chiral band states and because of potential applications. The low-energy quasiparticle excitation energies in graphene are linearly dispersing, described by Dirac cones at the edges of the first Brillouin zone.

Stable nonreactive graphene layers on top of ferromagnetic materials[9] might be used as sources of spin-polarized electrons. Electron sources are used in all domains ranging from technical devices like cathode-ray tubes to large scale scientific experiments like electron accelerators. This is of great interest for studies of magnetic systems in condensed matter physics, including the field of spintronics.

Graphene's spin-transport properties are expected to be particularly interesting, with predictions for extremely long coherence times and intrinsic spin-polarized states at zero field.[10] Spin-polarized electron emission from the graphene/Ni system before and after exposure to oxygen has been recently studied[11] and the study of spin polarization of secondary electrons obtained from this system upon photoemission suggested the use of passivated Ni surfaces as a source of spin-polarized electrons, since it is stable against adsorption of reactive gases. The spin-resolved transport has already been measured from conductance features by means of quantum interference.[12] These features split visibly in an in-plane magnetic field, similar to Zeeman splitting in atomic and quantum-dot systems. As a result, spin-up and spin-down conductance contributions at finite field are offset in gate voltage, leading to Zeeman splitting of interference features in a gate voltage.[12]

Many electronic and optical properties of graphene could be explained within a single-particle picture in which electron-electron interactions are completely neglected. The discovery of the fractional quantum Hall effect in graphene[13] represents an important hallmark in this context. By now, there is a large body of experimental work[8,14,15] showing the relevance of electron-electron interactions in a number of key properties of graphene samples of sufficiently high quality.

Conventional two-dimensional electron gas (2DEG), on the other hand, has been a fertile source of surprising new physics for more than four decades. Although graphene was only isolated for the first time in 2004 and it is still at an early stage, it is already clear[16] that the strong-field properties of Dirac electrons in graphene are different from and as rich as those of a semiconductor heterojunction 2DEG. The Fermi liquid phenomenology of Dirac electrons in graphene[4,5] and conventional 2DEG[17] have the same structure, since both systems are isotropic and have a single circular Fermi surface. The strength of interaction effects in a conventional 2DEG increases with decreasing carrier density. At low densities, the quasiparticle weight Z is small, the velocity is suppressed,[17] the charge compressibility changes sign from positive to negative, and the spin-susceptibility is strongly enhanced.[18] These effects emerge from an interplay between exchange interactions and quantum fluctuations of charge and spin in the 2DEG.

In addition, effective mass, or effective Fermi velocity, is an important concept in Landau's Fermi liquid theory since it provides a direct measure of the many-body interactions in the electron system. In the highly interacting, dilute, paramagnetic regime in the 2DEG the effective Fermi velocity, which is defined by the effective mass as $v^* = \hbar k_F/m^*$, is significantly diminished compared to its band value and tends to decrease with increasing r_s,[17–20] the so-called Wigner-Seitz radius. Recent measurements of the effective mass for electrons in two dimensions confined to AlAs quantum wells revealed that, when the 2DES is fully valley- and spin-polarized, the effective mass is suppressed down to values near or even slightly below the band mass.[19,21–23] A sophisticated theoretical calculation has been shown[24] that in an interacting, fully spin-polarized 2DES the absence (freezing out) of spin fluctuations reduces the effective mass below its band value, in agreement with experimental data. Furthermore, the spin-up and spin-down effective masses from magnetotransport measurements at different temperatures for a 2DEG and the effective hole mass

measurements through analyzing the temperature dependence of Shubnikov-de Haas oscillations in dilute 2D hole systems have been recently reported.[25]

In the Dirac electrons in graphene, it was shown[3–5,26] that interaction effects also become noticeable with decreasing density in that the quasiparticle weight Z tends to larger values, the velocity is enhanced rather than suppressed, and the influence of interactions on the compressibility and the spin susceptibility changes sign. These qualitative differences are due to *exchange interactions* between electrons near the Fermi surface and electrons in the negative energy sea and to interband contributions to Dirac electrons from charge and spin fluctuations.

Our aim in this work is to study the spin polarization dependence of quasiparticle properties in graphene, particulary, the renormalized velocity and inelastic scattering lifetime of quasiparticles within the leading-order single-loop self-energy expansion. Our theory for spin polarization dependence of quasiparticle velocity renormalization in interacting Dirac electron systems is motivated not only by fundamental many-body considerations, but also by the possibility to improve high-speed operation in spintronic devices[27] and potential future experiments. By chemical doping in graphene, spin polarization effects are predicted for some adsorption configurations.[28] Remarkably, the studies of spin polarization dependence of quasiparticle properties should help to understand spin valve physics and recent measurements of electronic spin transport in graphene,[29] and the possibility of magnetism in graphene induced by single carbon atom defects.[30]

The paper is organized as the following. In Sec. II, we introduce a formalism that will be used in calculating spin-polarization quasiparticle properties, which includes the many-body effects by suing RPA. In Sec. III, we present our analytical and numerical results for the self-energy and renormalized Fermi velocity in doped graphene sheets. Section IV contains discussions and conclusions.

II. METHOD AND THEORY

We consider the long-range Coulomb electron-electron interaction. We left out the intervalley scattering and use the two-component Dirac Fermion model. Accordingly, the total interacting Hamiltonian in a continuum model at K^+ point is expressed as[31]

$$\hat{H} = -i\hbar v \sum_i \vec{\sigma}\cdot\nabla_i + \frac{1}{2}\sum_{i\neq j} V(\mathbf{r}_i - \mathbf{r}_j), \qquad (1)$$

where $\vec{\sigma}$ are Pauli matrices and $v = 3ta/2\hbar \simeq 10^6$ m/s is the Fermi velocity with $a \simeq 1.42$ Å is the carbon-carbon distance in honeycomb lattice. Here, $\mathbf{p}_i = -i\hbar\nabla_i$ is the canonical momentum of the ith electron and $v_q = 2\pi e^2/\epsilon q$ is the Fourier transform of the bare Coulomb interaction where ϵ is an average dielectric constant of the surrounding medium. The coupling constant in graphene or graphene's fine-structure constant is $\alpha_{ee} = e^2/\epsilon\hbar v$. The coupling constant in graphene depends only on the substrate dielectric constant while in the conventional 2D electron systems is density dependent. The typical value of dimensionless coupling constant is 0.25 or 0.5 for graphene supported on a substrate such as SiC or SiO_2.

As it is clearly seen from the first term of Eq. (1), the spectrum is unbounded from below and it implies that the Hamiltonian has to be accompanied by an ultraviolet cutoff, which is defined by k_c and it should be assigned a value corresponding to the wave-vector range over which the continuum model (1) describes graphene. For definiteness, we take k_c to be such that $\pi k_c^2 = 2(2\pi)^2/\mathcal{A}_0$, where $\mathcal{A}_0 = 3\sqrt{3}a_0^2/2$ is the area of the unit cell in the honeycomb lattice. With this choice, the energy $\hbar v k_c = 7$ eV and

$$\Lambda = \frac{k_c}{k_F} = \sqrt{\frac{2g_v}{n\mathcal{A}_0}}. \qquad (2)$$

The continuum model is useful when $k_c \gg k_F$, i.e., when $\Lambda \gg 1$. Note that, for instance, electron densities $n = 0.36\times 10^{12}$ and 0.36×10^{14} cm^{-2} correspond to $\Lambda = 100$ and 10, respectively.

The spin-polarization dependence of dynamical polarizability tensor in terms of one-body noninteracting Green's function is written as[32]

$$\chi_\sigma^{(0)}(\mathbf{q},\Omega,\mu) = -i\int\frac{d^2\mathbf{k}}{(2\pi)^2}\int\frac{d\omega}{2\pi} \mathrm{Tr}\big[i\gamma_0 G_\sigma^{(0)}(\mathbf{k}+\mathbf{q},\omega+\Omega,\mu) i\gamma_0 G_\sigma^{(0)}(\mathbf{k},\omega,\mu)\big], \qquad (3)$$

where σ refers to the spin-direction, $\uparrow$ or $\downarrow$. After implementing $G_\sigma^{(0)}(\mathbf{k},\omega,\mu)$ in Eq. (3) and calculating the integral, the results end up to be[3]

$$\chi_\sigma^{(0)}(\mathbf{q},i\Omega,\mu) = -g_v\frac{\mu^\sigma}{2\pi v^2} - g_v\pi B/2 + g_v B\Re e[\arcsin(C) + C\sqrt{1-C^2}], \qquad (4)$$

where $g_v = 2$ is valley degeneracy. μ^σ is the spin dependence chemical potential, $B = q^2/(8\pi\sqrt{\Omega^2+v^2q^2})$, and $C = (2\mu^\sigma + i\Omega)/(vq)$.

The technical calculation[32] on which our conclusions are based is an evaluation of the spin-polarization dependence electron self-energy $\Sigma_s^\sigma(\mathbf{k},\omega)$ of the Dirac fermion near the quasiparticle pole. $\Sigma_s^\sigma(\mathbf{k},\omega)$ describes the interaction of a single Dirac electron with spin σ near the 2D Fermi surface with all states inside the Fermi sea, and with virtual particle-hole and collective excitations of the entire Fermi sea. A direct expansion of electron self-energy in powers of the Coulomb interaction is never possible in a 2D electron liquid because of the long-range of the Coulomb interaction. Our results for the Dirac electron gas are based on the random phase approximation (RPA) in which the self-energy is expanded to the first order in the dynamically screened Coulomb interaction (setting $\hbar = 1$):

$$\Sigma_s^\sigma(\mathbf{k},i\omega_n) = -\frac{1}{\beta}\sum_{s'}\int\frac{d^2\mathbf{q}}{(2\pi)^2}\sum_{m=-\infty}^{+\infty}\frac{v_q}{\varepsilon(\mathbf{q},i\Omega_m,\zeta)} \times\left[\frac{1+ss'\cos(\theta_{\mathbf{k},\mathbf{k}+\mathbf{q}})}{2}\right] G_{s'}^{0\sigma}(\mathbf{k}+\mathbf{q},i\omega_n+i\Omega_m), \qquad (5)$$

where $s = +$ for electron-doped systems and $s = -$ for hole-doped systems, ζ is the spin polarization parameter, $\zeta = |n_\uparrow - n_\downarrow|/n$, $\beta = 1/(k_B T)$, and $\varepsilon(\mathbf{q},i\Omega_m,\zeta)$ is the RPA dielectric

function. n_σ is the spin-polarized density and n is the total density of the system. The RPA dielectric function is given by

$$\varepsilon(\mathbf{q},i\Omega,\zeta) = 1 - v_q[\chi_\uparrow^{(0)}(\mathbf{q},i\Omega,\zeta) + \chi_\downarrow^{(0)}(\mathbf{q},i\Omega,\zeta)]. \quad (6)$$

In the Dirac 2D electron system, dielectric-function contributions from intraband and interband excitations are subtly interrelated. The two contributions must be included on an equal footing in order to describe the Dirac fermion physics correctly. For example, one key property, that the static dielectric function is independent of q at small q, requires intraband and interband contributions to be summed.

For definiteness, we limit our discussion to an electron-doped system with spin polarization dependence of chemical potential μ^σ. In Eq. (5), $\omega_n = (2n+1)\pi/\beta$ is a fermionic Matsubara frequency, the sum runs over all the bosonic Matsubara frequencies $\Omega_m = 2m\pi/\beta$. The factor in square brackets in Eq. (5), which depends on the angle $\theta_{\mathbf{k},\mathbf{k}+\mathbf{q}}$ between $\mathbf{k}$ and $\mathbf{k}+\mathbf{q}$, captures the dependence of Coulomb scattering on the relative chirality ss' of the interacting electrons. The Green's function $G_s^{0\sigma}(\mathbf{k},i\omega) = 1/[i\omega - \xi_s^\sigma(\mathbf{k})]$ describes the free propagation of states with wave vector $\mathbf{k}$, Dirac energy $\xi_s^\sigma(\mathbf{k}) = svk - \mu^\sigma$ (relative to the chemical potential) and chirality $s = \pm$. The quasiparticle excitation energy measured from the chemical potential can be given by Dyson equation $E_s^\sigma(\mathbf{k}) = \xi_s^\sigma(\mathbf{k}) + \Re e\Sigma_s^{(\mathrm{ret},\sigma)}(\mathbf{k},\omega)$ evaluated at $\omega = E_s^\sigma(\mathbf{k})$. After continuation from imaginary to real frequencies, $i\omega \to \omega + i\eta$ and using the Dyson equation, the spin-dependent renormalized Fermi velocity can be expressed[32] in terms of the wave vector and frequency derivatives of the retarded self-energy $\Sigma_+^{(\mathrm{ret},\sigma)}(\mathbf{k},\omega)$ evaluated at the spin-dependent Fermi surface, which is $k_F^\sigma = (1+\sigma\zeta)^{1/2}k_F$, where k_F is the Fermi momentum:

$$\frac{v_\sigma^{\star(\mathrm{Dyson})}}{v} = \frac{dE_+^\sigma(\mathbf{k})}{d\mathbf{k}} = \frac{1 + (v)^{-1}\partial_k \Re e\Sigma_+^{(\mathrm{ret},\sigma)}(\mathbf{k},\omega)|_{k=k_F^\sigma,\omega=0}}{1 - \partial_\omega \Re e\Sigma_+^{(\mathrm{ret},\sigma)}(\mathbf{k},\omega)|_{k=k_F^\sigma,\omega=0}}. \quad (7)$$

In the on-shell approximation (OSA), on the other hand, the renormalized velocity is given by

$$\frac{v_\sigma^{\star(\mathrm{OSA})}}{v} = 1 + (v)^{-1}\partial_k \Re e[\Sigma_+^{(\mathrm{ret},\sigma)}(\mathbf{k},\omega)]|_{\omega=0,k=k_F^\sigma} + \partial_\omega \Re e[\Sigma_+^{(\mathrm{ret},\sigma)}(\mathbf{k},\omega)]|_{\omega=0,k=k_F^\sigma}. \quad (8)$$

This expression can also be obtained from the formal definition of v^* given in the first equality in Eq. (7) when the second term in the Dyson equation, $\Re e\Sigma_+^{(\mathrm{ret},\sigma)}(\mathbf{k},\omega)$, is evaluated at the bare pole, $\omega = \xi_+^\sigma(\mathbf{k})$. The OSA thus gives the quasiparticle velocity to the first order in the retarded self-energy. The renormalized velocity in this approximation demonstrates qualitatively the same behavior obtained by the Dyson equation, Eq. (7), but its magnitude is larger than the one calculated within the Dyson scheme.

The quasiparticle weight factor Z_σ evaluated at the spin-dependent Fermi surface and given by $Z_\sigma^{-1} = 1 - \partial_\omega \Re e\Sigma_+^{(\mathrm{ret},\sigma)}(\mathbf{k},\omega)|_{k=k_F^\sigma,\omega=0}$. In the up-spin case, the majority-spin, $Z_\uparrow$ value is a bit smaller and the down-spin case, the minority spin, $Z_\downarrow$ value is bigger than the results of $Z(\zeta = 0)$.

III. NUMERICAL RESULTS

Since the single-particle self-energy, the density of states, the dynamical screening, the Fermi momentum, and the Fermi energy in the chiral Dirac fermion are all affected by spin polarization, we expect all Fermi liquid parameters to be strongly dependent on the spin-polarization parameter. An important thermodynamic quantity is the system compressibility, which has been already studied by two of us.[33]

Our results for the spin-polarization dependence of the Dirac electron velocity $v^\star{}_\sigma/v$ at fixed electron density value in the up- and down-spin, the majority- and minority-spin as a function of the ζ are summarized in Fig. 1 for different values of the dimensionless coupling constant α_{ee}. For the up-spin Dirac electron, the renormalized velocity decreases with increasing spin-polarization degree of freedom. However, the down-spin electron renormalized velocity increases by increasing spin-polarization. These behaviors are based on the effect of the exchange energy in the spin channels between electrons near the Fermi surface. Since the electron density in the down-spin channel, $n_\downarrow = n(1-\zeta)/2$ is less than the electron density in the up-spin channel $n_\uparrow = n(1+\zeta)/2$, and

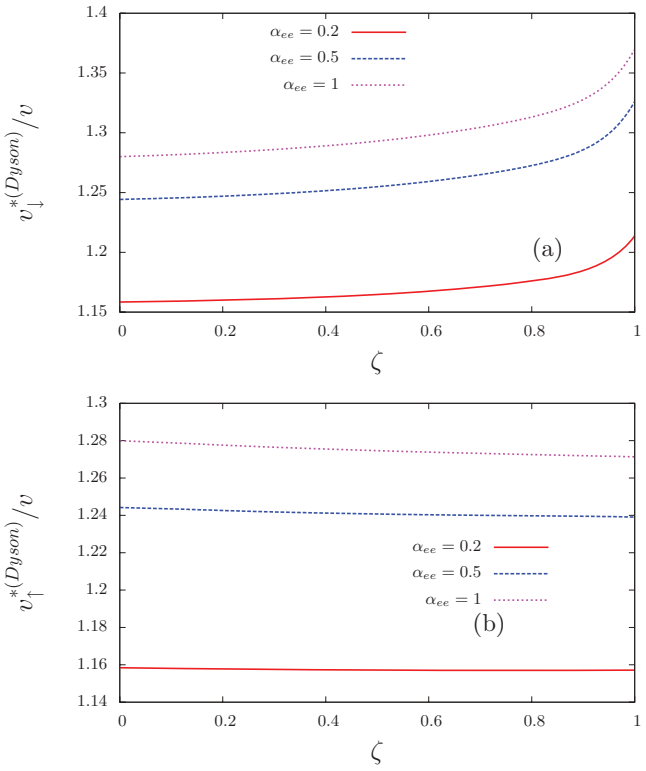

FIG. 1. (Color online) Spin-polarization dependence of the renormalized velocity, in the Dyson scheme, scaled by that of a noninteracting velocity as a function of the degree of spin polarization ζ for cutoff value $\Lambda = 100$ ($n = 0.36 \times 10^{12}$ cm^{-2}) in (a) the down-spin, where $0 < n_\downarrow < 0.18 \times 10^{12}$ cm^{-2}, and (b) the up-spin, where $0.18 \times 10^{12} < n_\uparrow < 0.36 \times 10^{12}$ cm^{-2}, for different coupling constant values. The spin polarization dependence of the up- and down-spin velocity behaves differently as ζ increases.

$n_\downarrow$ decreases, however, $n_\uparrow$ increases by increasing ζ, therefore the exchange contribution of the down-spin is dominated and results in increasing the renormalized velocity in the spin-down channel and decreasing the renormalized velocity in the spin-up channel. In contrast, the 2DEG where the down-spin mass increases with spin-polarization first and as ζ approaches near to one, it decreases sharply, the spin-polarized down-spin velocity tends to a constant when ζ reaches to unity.[34] It should be noticed that the up- and down-spin Fermi velocities have the same value at $\zeta = 0$.

As it has been discussed previously,[3–5] graphene's Fermi liquid properties depend only weakly on the carrier density, which is expressed in terms of the cutoff parameter Λ. The trends exhibited in Fig. 1 can be understood by considering the limits of small α_{ee} and the limit of large q at all values of α_{ee}. In the former limit, screening is weak except at extremely small q. The self-energy can be decomposed as the sum of a contribution from the interaction of quasiparticles at the Fermi energy, the *residue* contribution $\Sigma^{(\mathrm{res},\sigma)}$, and a contribution from interactions with quasiparticles far from the Fermi energy and via both exchange and virtual fluctuations, the *line* contribution $\Sigma^{(\mathrm{line},\sigma)}$. In $\partial_\omega \Sigma_+^{(\mathrm{res},\sigma)}(\mathbf{k},\omega)$, for example, the integral over q diverges logarithmically at small q when $\varepsilon(\mathbf{q},\omega=0)$ is set equal to one, i.e., when screening is neglected. Accordingly, screening cuts off this logarithmic divergence at a wave vector. More precisely, we have

$$\frac{\partial}{\partial\omega}\Sigma_+^{(\mathrm{res},\sigma)}(\mathbf{k},\omega)|_{k=k_F^\sigma,\omega=0} = \frac{\alpha_{ee}}{2\pi}\int_0^{2\sqrt{1+\sigma\zeta}} dx \frac{1}{x\varepsilon(x,0)}\frac{4-x^2/(1+\sigma\zeta)}{\sqrt{4-x^2/(1+\sigma\zeta)}}, \quad (9)$$

and notice that $\partial_\omega \Re e\,\Sigma_+^{(\mathrm{res},\sigma)}(k_\mathrm{F},0) = 0$ for a case that $\sigma\zeta = -1$. Because $\varepsilon(\mathbf{q},\omega=0)$ happens to be independent of q for transitions between Fermi surface points, it is possible to evaluate $\partial_\omega \Sigma_+^{(\mathrm{res},\sigma)}(\mathbf{k},\omega)$ for the case that $\sigma\zeta \neq -1$ analytically. We find that

$$\frac{\partial}{\partial\omega}\Re e\,\Sigma_+^{(\mathrm{res},\sigma)}(k_\mathrm{F},\omega=0) = \frac{\alpha_{ee}}{2\pi}\left[\sqrt{4-\eta_\sigma^2}\,\ln\left(\frac{2+\sqrt{4-\eta_\sigma^2}}{\eta_\sigma}\right) - \frac{1}{2}(4-\eta_\sigma\pi)\right], \quad (10)$$

where $\eta_\sigma = g_v\alpha_{ee}(\sqrt{1+\zeta}+\sqrt{1-\zeta})/\sqrt{1+\sigma\zeta}$. It should be worthwhile mentioning that for $\eta_\sigma > 2$ we use an equality in which $-i\ln(x+i\sqrt{1-x^2}) = \arccos(x)$ when $x \leqslant 1$. Importantly, similar ζ dependence appears in the v_σ^* at small α_{ee}. More precisely, the ζ dependence of $v_\sigma^*(\zeta)$, both in the Dyson and OSA schemes, in the $\alpha_{ee} \to 0$ limit, for $\zeta < 1$, is given by

$$\frac{v_\sigma^*(\zeta)}{v} - 1 = \frac{\alpha_{ee}}{\pi}\left[\ln(g_v\alpha_{ee}) + \ln\left(\frac{\eta_\sigma}{2\alpha_{ee}}\right)\right]. \quad (11)$$

This analytical expression shows that the renormalized velocity in the down-spin enhances while it decreases in the up-spin channel. In the limit of small ζ, Eq. (11) is simplified and $v_{\uparrow\downarrow}^*(\zeta)/v - 1 = \alpha_{ee}[\ln(g_v\alpha_{ee}) \mp \zeta/2]/\pi$. All these behaviors are very familiar from the case of the effective mass or the effective Fermi velocity in a normal 2DES but more significantly, the spin-polarization term is different than that of the 2DEG.[34,35] The discrepancy is due to the nature of the chiral Dirac electron behavior in graphene flake having the linear dispersion relation.

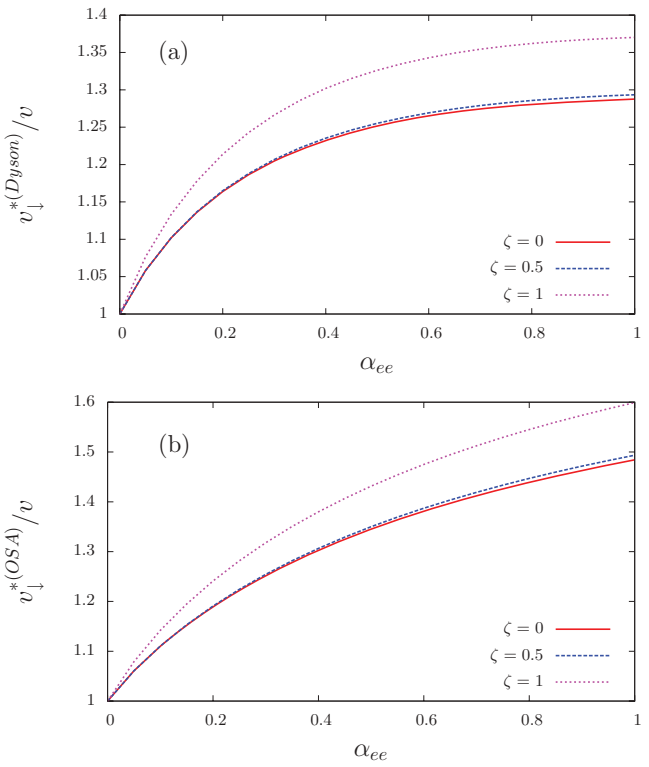

FIG. 2. (Color online) Renormalized velocity of the down-spin scaled by that of a noninteracting velocity, $v_\downarrow^*/v$, as a function of the coupling constant α_{ee} for cutoff value $\Lambda = 100$ ($n = 0.36 \times 10^{12}$ cm^{-2}) in (a) Dyson and (b) OSA approximations given by Eqs. (7) and (8), respectively.

In Fig. 2, we show the down-spin renormalized velocity scaled by that of a noninteracting velocity as a function of the coupling constant in both the Dyson and OSA approximations, which are defined by Eqs. (7) and (8), respectively. Clearly, the velocity values increase significantly when ζ approaches to unity. Despite the strong down-spin velocity dependence of the spin degree of freedom, the up-spin velocity becomes smoothly smaller with ζ as it is shown in Fig. 3. Notice that $v_\sigma^{*(\mathrm{OSA})}$ is always larger than $v_\sigma^{*(\mathrm{Dyson})}$. Moreover, the ζ dependence of the renormalized velocity is opposite with respect to the spin direction. It would be worthwhile finding the asymptotic behavior of v_σ^* at some conditions. At large q, interband charge fluctuations dominate $\varepsilon(\mathbf{q},\omega) - 1$, which approaches its simple undoped system form. It becomes especially clear when ω is expressed in units of vq that the typical value of $\varepsilon(\mathbf{q},\omega)$ at large q is $\sim$1 with a nontrivial dependence on α_{ee}. The q integrals all vary as q^{-1}, requiring that the Dirac electrons model be accompanied by an ultraviolet cutoff. Since the crossover between intraband and interband screenings occurs for $q \sim k_\mathrm{F}$, it follows that $\partial_k \Sigma^{\mathrm{res}}$ and $\partial_\omega \Sigma^{\mathrm{res}}$ have contributions that are analytic in α_{ee} and vary as $\ln(\Lambda)$ when Λ is large. To leading order in $\ln(\Lambda)$, we find that $v^\star/v - 1 = \alpha_{ee}[1 - 2g_v\alpha_{ee}g(2g_v\alpha_{ee})]\ln(\Lambda)/4$, which is σ independent and $g(x)$ is defined in Ref. 4.

In Fig. 4, we show the down-spin renormalized velocity as a function of the electron density (in units of 10^{12} cm^2).

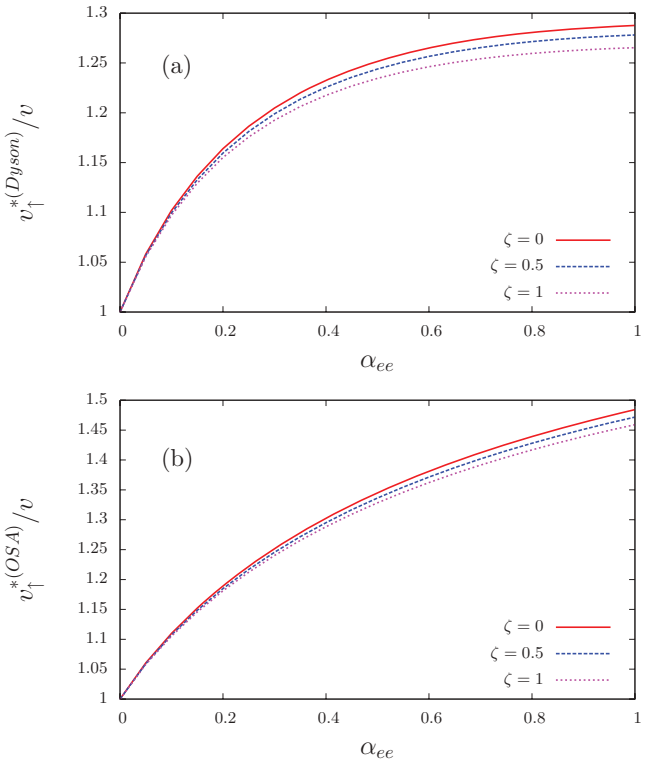

FIG. 3. (Color online) Renormalized velocity of the up-spin scaled by that of a noninteracting velocity, $v_\uparrow^*/v$, as a function of the coupling constant α_{ee} for cutoff value $\Lambda = 100$ ($n = 0.36 \times 10^{12}$ cm^{-2}) in (a) Dyson and (b) OSA approximations given by Eqs. (7) and (8), respectively.

In contrast to the 2DEG, the renormalized velocity increases by decreasing the electron density and indicates no Wigner crystallization[32] occurs in pristine Dirac fermion systems.[36] Note that at very small n, the system is highly correlated and a model going beyond the RPA is necessary to account for increasing correlation effects at low density.[37] Our theoretical calculations show that, even at moderately low densities, the velocity enhancement in a supported graphene sheet can vary a lot in qualitatively good agreement with measured data in a suspended graphene sheet.[26]

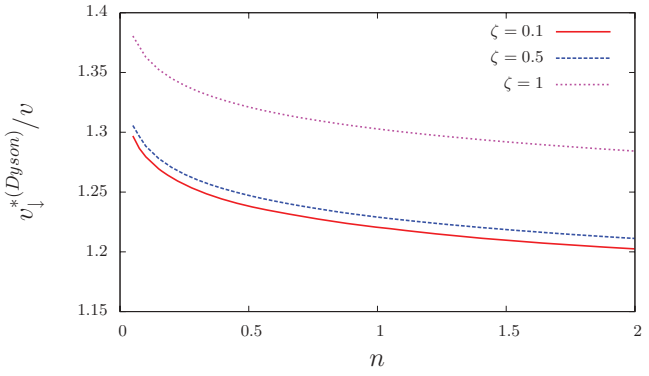

FIG. 4. (Color online) Renormalized velocity of the down-spin, in the Dyson scheme, scaled by that of a noninteracting velocity as a function of the electron density (in units of 10^{12} cm^{-2}) for different ζ values at $\alpha_{ee} = 0.5$.

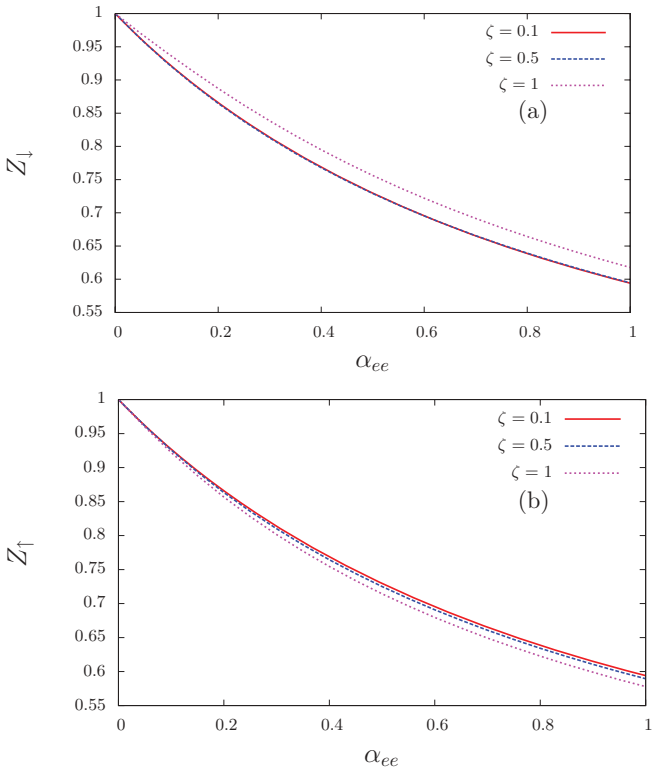

FIG. 5. (Color online) Renormalized constant Z_σ for (a) the down spin and (b) the up spin as a function of the coupling constant α_{ee} for cutoff value $\Lambda = 100$ ($n = 0.36 \times 10^{12}$ cm^{-2}).

We have also calculated the renormalization factor $Z_\sigma(\alpha_{ee},\zeta)$, which is equal to the discontinuity in the momentum distribution at k_F^σ. The effect of ζ is to make the $Z_\downarrow$ values larger at large α_{ee} compared to the case when ζ is not included as shown in Fig. 5. The nonzero values of Z_σ, shows the Fermi liquid picture in the whole range of α_{ee} and ζ. When $n \to 0$ the Z_σ factor drops to zero logarithmically. Notice that in leading order of $\ln\Lambda$, the renormalization factor is independent of σ and behaves like $Z^{-1} - 1 = \alpha_{ee}\lambda(2g_v\alpha_{ee})\ln(\Lambda)/6$ where $\lambda(x)$ is defined in Ref. 4.

Finally, we compute the inelastic scattering lifetime of quasiparticles due to carriers-carriers interactions at zero temperature for different ζ values. This is obtained through the imaginary part of the self-energy when the frequency evaluated at the on-shell energy,

$$\tau_{\rm in}^{\sigma\,-1}(\mathbf{k}) = \Gamma_{\rm in}^\sigma(\mathbf{k}) = -\frac{2}{\hbar}\Im m\,\Sigma_+^{({\rm ret},\sigma)}(\mathbf{k},\xi_+^\sigma(\mathbf{k}/\hbar)), \qquad (12)$$

where $\Gamma_{\rm in}^\sigma(\mathbf{k})$ is the quantum level broadening of the momentum with eigenstate $|\mathbf{k}\rangle$. It is worthwhile to note that the expression of $\tau_{\rm in}^{\sigma\,-1}(\mathbf{k})$ is identical with a result obtained by the Fermi's golden rule summing the scattering rate of electron and hole contributions at wave vector $\mathbf{k}$.[32] Figure 6 shows the behavior of the spin polarization dependence of the inverse inelastic scattering lifetime for $n = 5 \times 10^{12}$ cm^{-2} and $\alpha_{ee} = 0.25$. The imaginary part of the self-energy evaluated at the on-shell energy starts from $\xi_+^\sigma(k) = -\varepsilon_{\rm F}^\sigma$, exhibits a minimum at zero energy and then grows up. The scattering rate in graphene is a smooth function, which is in contrast with the conventional 2D semiconductors and 2D electron liquids

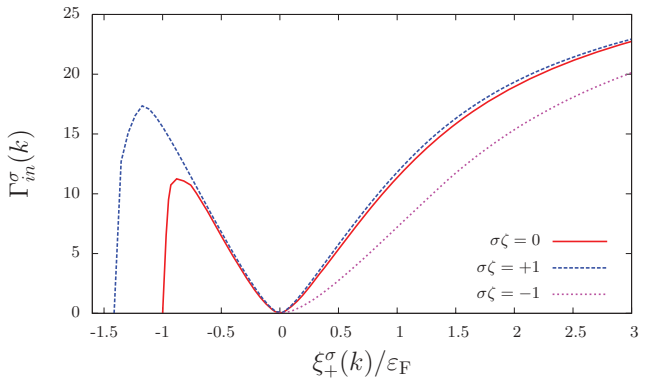

FIG. 6. (Color online) Inverse inelastic scattering lifetime of quasiparticle, $\Gamma^{\sigma}_{\rm in}(k)$ (in units of psec^{-1}) in graphene as a function of the on-shell energy, $\xi^{\sigma}_{+}(k)$ for different spin polarization values. The data in this figure refer to $n = 5 \times 10^{12}$ cm^{-2} and $\alpha_{ee} = 0.25$.

because of the absence of both plasmon emission and interband processes.[38] We also see in Fig. 6 that the scattering rate is quite sensitive to the spin polarization and the inelastic lifetime for minority spins is larger evidently than the majority spin lifetime. The ratio of the majority- to minority-spin lifetime is smaller than unity and related directly to the polarization and electron energy.

IV. CONCLUSIONS

In summary, we have calculated the spin-polarized dependence of the quasiparticle in graphene sheets and they could be strongly spin-polarization dependent and substantially different than the usual unpolarized paramagnetic values. Similar to a two-dimensional paramagnetic diluted magnetic semiconductor electron gas,[39] the Dirac electron Fermi velocity is highly spin dependent even if the spin polarization of the carrier population is negligibly small. Therefore, the spin-polarization dependence of chiral carrier transports can be observed experimentally nearly full spin polarization regimes. The majority-spin electron renormalized velocity decreases with increasing spin-polarization degree of freedom. However, the minority-spin electron renormalized velocity increases by increasing spin polarization due to reduction in the electron density and consequently increase in the interaction between electrons near the Fermi surface. We show that the ratio of the lifetimes of majority- to minority-spin electrons is smaller than unity and related to the polarization and electron energy. It has important implications for the interpretation of many types of spin-polarized experiments. Our results might be used in calculating the effective density of states in graphene spintronic systems. The spin-polarized features that are the subject of this work may, in the future, lead to the development of graphene devices incorporating interference-based spin filters.

ACKNOWLEDGMENT

We would like to thank M. Polini for useful discussions. A.Q. was supported by EU-ICT-7 contract No. 257159 "MACALO."

*asgari@ipm.ir

[1] K. S. Novoselov, A. K. Geim, S. V. Morozov, D. Jiang, Y. Zhang, S. V. Dubonos, I. V. Grigorieva, and A. A. Firsov, Science **306**, 666 (2004).

[2] A. K. Geim and A. H. MacDonald, Phys. Today **60**, 35 (2007); A. K. Geim and K. S. Novoselov, Nat. Mater. **6**, 183 (2007).

[3] Y. Barlas, T. Pereg-Barnea, M. Polini, R. Asgari, and A. H. MacDonald, Phys. Rev. Lett. **98**, 236601 (2007).

[4] M. Polini, R. Asgari, Y. Barlas, T. Pereg-Barnea, and A. H. MacDonald, Solid State Commun. **143**, 58 (2007).

[5] M. Polini, R. Asgari, G. Borghi, Y. Barlas, T. Pereg-Barnea, and A. H. MacDonald, Phys. Rev. B **77**, 081411(R) (2008); E. H. Hwang and S. Das Sarma, *ibid.* **77**, 081412 (2008).

[6] Fernando de Juan, Adolfo G. Grushin, and Maria A. H. Vozmediano, Phys. Rev. B **82**, 125409 (2010); Paolo E. Trevisanutto, Christine Giorgetti, Lucia Reining, Massimo Ladisa, and Valerio Olevano, Phys. Rev. Lett. **101**, 226405 (2008); R. Roldán, M. P. López-Sancho, and F. Guinea, Phys. Rev. B **77**, 115410 (2008).

[7] R. Asgari, M. M. Vazifeh, M. R. Ramezanali, E. Davoudi, and B. Tanatar, Phys. Rev. B **77**, 125432 (2008).

[8] Valeri N. Kotov, Bruno Uchoa, Vitor M. Pereira, A. H. Castro Neto, and F. Guinea, arXiv:1012.3484.

[9] Yu. S. Dedkov, A. M. Shikin, V. K. Adamchuk, S. L. Molodtsov, C. Laubschat, A. Bauer, and G. Kaindl, Phys. Rev. B **64**, 035405 (2001); D. Farias, A. M. Shikin, and K.-H. Rieder, and Yu. S. Dedkov, J. Phys.: Condens. Matter **11**, 8453 (1999); A. M. Shikin, G. V. Prudnikova, V. K. Adamchuk, F. Moresco, and K.-H. Rieder, Phys. Rev. B **62**, 13202 (2000).

[10] O. V. Yazyev, Nano Lett. **8**, 1011 (2008); C. L. Kane and E. J. Mele, Phys. Rev. Lett. **95**, 226801 (2005); N. M. R. Peres, F. Guinea, and A. H. Castro Neto, Phys. Rev. B **72**, 174406 (2005); M. Wimmer, I. Adagideli, S. Berber, D. Tománek, and K. Richter, Phys. Rev. Lett. **100**, 177207 (2008).

[11] Yu. S. Dedkov, M. Fonin, and C. Laubschat, Appl. Phys. Lett. **92**, 052506 (2008).

[12] Mark B. Lundeberg and Joshua A. Folk, Nat. Phys. **5**, 894 (2009).

[13] X. Du, I. Skachko, F. Duerr, A. Luican, and E. Y. Andrei, Nature (London) **462**, 192 (2009); Kirill I. Bolotin, Fereshte Ghahari, Michael D. Shulman, Horst L. Stormer, and Philip Kim, *ibid.* **462**, 196 (2009).

[14] V. W. Brar *et al.*, Phys. Rev. Lett. **104**, 036805 (2010); E. A. Henriksen, P. Cadden-Zimansky, Z. Jiang, Z. Q. Li, L.-C. Tung, M. E. Schwartz, M. Takita, Y.-J. Wang, P. Kim, and H. L. Stormer, *ibid.* **104**, 067404 (2010); A. Luican, G. Li, and E. Y. Andrei, Phys. Rev. B **83**, 041405(R) (2011); K. F. Mak, J. Shan, and T. F. Heinz, *ibid.* **106**, 046401 (2011); Fereshte Ghahari, Yue Zhao, Paul Cadden-Zimansky, Kirill Bolotin, and Philip Kim, *ibid.* **106**, 046801 (2011).

[15] A. Bostwick, F. Speck, T. Seyller, K. Horn, M. Polini, R. Asgari, A. H. MacDonald, and E. Rotenberg, Science **328**, 999 (2010).

[16]M. O. Goerbig, Rev. Mod. Phys. **83**, 1193 (2011); K. S. Novoselov, A. K. Geim, S. V. Morozov, D. Jiang, M. I. Katsnelson, I. V. Grigorieva, S. V. Dubonos, and A. A. Firsov, Nature (London) **438**, 197 (2005).

[17]R. Asgari and B. Tanatar, Phys. Rev. B **74**, 075301 (2006).

[18]R. Asgari, B. Davoudi, M. Polini, G. F. Giuliani, M. P. Tosi, and G. Vignale, Phys. Rev. B **71**, 045323 (2005).

[19]M. Padmanabhan, T. Gokmen, N. C. Bishop, and M. Shayegan, Phys. Rev. Lett. **101**, 026402 (2008).

[20]R. Asgari, B. Davoudi, and B. Tanatar, Solid State Commun. **130**, 13 (2004).

[21]S. Gangadharaiah and D. L. Maslov, Phys. Rev. Lett. **95**, 186801 (2005).

[22]T. Gokmen, M. Padmanabhan, and M. Shayegan, Phys. Rev. Lett. **101**, 146405 (2008).

[23]T. Gokmen, M. Padmanabhan, K. Vakili, E. Tutuc, and M. Shayegan, Phys. Rev. B **79**, 195311 (2009).

[24]R. Asgari, T. Gokmen, B. Tanatar, M. Padmanabhan, and M. Shayegan, Phys. Rev. B **79**, 235324 (2009).

[25]L. M. Wei, K. H. Gao, X. Z. Liu, W. Z. Zhou, L. J. Cui, Y. P. Zeng, G. Yu, R. Yang, T. Lin, L. Y. Shang, S. L. Guo, N. Dai, J. H. Chu, and D. G. Austing, J. Appl. Phys. **110**, 063707 (2011); Y. T. Chiu, M. Padmanabhan, T. Gokmen, J. Shabani, E. Tutuc, M. Shayegan, and R. Winkler, Phys. Rev. B **84**, 155459 (2011).

[26]D. C. Elias, R. V. Gorbachev, A. S. Mayorov, S. V. Morozov, A. A. Zhukov, P. Blake, L. A. Ponomarenko, I. V. Grigorieva, K. S. Novoselov, F. Guinea, and A. K. Geim, Nat. Phys. **7**, 701 (2011).

[27]Sungjae Cho, Yung-Fu Chen, and Michael S. Fuhrer, Appl. Phys. Lett. **91**, 123105 (2007).

[28]I. Zanella, S. Guerini, S. B. Fagan, J. Mendes Filho, and A. G. Souza Filho, Phys. Rev. B **77**, 073404 (2008).

[29]Nikolaos Tombros, Csaba Jozsa, Mihaita Popinciuc, Harry T. Jonkman, and Bart J. van Wees, Nature (London) **448**, 571 (2007).

[30]Oleg V. Yazyev and Lothar Helm, Phys. Rev. B **75**, 125408 (2007); V. M. Pereira, J. M. B. Lopes dos Santos, and A. H. Castro Neto, *ibid*. **77**, 115109 (2008).

[31]J. C. Slonczewski and P. R. Weiss, Phys. Rev. **109**, 272 (1958); T. Ando, T. Nakanishi, and T. Saito, J. Phys. Soc. Jpn. **67**, 2857 (1998).

[32]G. F. Giuliani and G. Vignale, *Quantum Theory of the Electron Liquid* (Cambridge University Press, Cambridge, 2005).

[33]A. Qaiumzadeh and R. Asgari, Phys. Rev. B **80**, 035429 (2009).

[34]Ying Zhang and S. Das Sarma, Phys. Rev. Lett. **95**, 256603 (2005).

[35]Note that the effective mass in 2DEG at small r_s and ζ values behaves like $m^*_{\uparrow\downarrow}/m = 1 + (r_s/\sqrt{2}\pi)\ln r_s \mp (r_s\zeta/2\sqrt{2}\pi)\ln r_s$.

[36]Hari P. Dahal, Yogesh N. Joglekar, Kevin S. Bedell, and Alexander V. Balatsky, Phys. Rev. B **74**, 233405 (2006).

[37]S. Das Sarma, E. H. Hwang, and Wang-Kong Tse, Phys. Rev. B **75**, 121406 (2007).

[38]A. Qaiumzadeh, F. Joibari, and R. Asgari, Eur. Phys. J. B **74**, 749 (2010); E. H. Hwang, Ben Yu-Kuang Hu, and S. Das Sarma, Phys. Rev. B **76**, 115434 (2007).

[39]W. Yang, Kai Chang, X. G. Wu, and H. Z. Zheng, App. Phys. Lett. **88**, 082107 (2006).